Geotechnical Aspects of Underground Construction in Soft Ground, Kusakabe, Fujita & Miyazaki (eds)

Development of a ground reaction curve for shield tunnelling

A. Sramoon & M. Sugimoto
Nagaoka University of Technology, Niigata, Japan

ABSTRACT: The change of ground deformation is the main cause of earth pressure change around shield periphery during excavation. The ground deformation can be calculated based on shield behaviour and excavation condition. The earth pressure acting on the shield periphery caused by ground displacement could be estimated by applying the ground reaction curve. The ground reaction curve, which is the relationship between the ground deformation and the earth pressure, was developed based on 2-D finite element analysis of shield tunnelling. The reasonable agreement of earth pressure acting on shield between the proposed ground reaction curve and the observation data was reported. This agreement for the earth pressure acting on shield suggested that the proposed ground reaction curve could be applied to the shield behaviour model and the segment design.

1 INTRODUCTION

The earth pressure acting on the shield or lining changes in accordance with the ground displacement along the tunnel at the difference stage of excavation. When the ground displacement around the tunnel occurs inwardly inside the tunnel, the earth pressure decreases in proportion to the degree of displacement, that is, active earth pressure. In contrast, when the displacement of ground around the tunnel appears outward from the tunnel, the earth pressure becomes passive. The earth pressure acting on the tunnel is determined not only by the tunnel shape and the characteristic of the ground but also by many other factors, such as the excavation method, the control of shield, the stiffness and the erection timing of the lining, the grouting method and the ground water conditions.

In this study, focusing on the earth pressure acting on shield, the shield movement is considered to have the snake motion as shown in Figure 1. The active earth pressure occurs when the ground at open face deforms towards the shield periphery. The void between the excavated area and the outer skin plate of shield is caused by over-excavation of the cutter face or copy cutter. On the other hand, as the shield has travels within the excavated area, some part of it pushes the ground, and that creates the passive earth pressure. This situation is caused by the control of the shield related with the applied jack thrust and the shield movement direction.

A ground reaction curve has been developed to cope with the relationship between the earth pressure acting on shield periphery and the ground displacement, which is significantly affected by shield tunnel alignment control during excavation. The method to determine the parameters in the ground reaction curve, based on finite element analysis, has also been established. Furthermore, the proposed ground reaction curve was examined by comparing the results with the observation data.

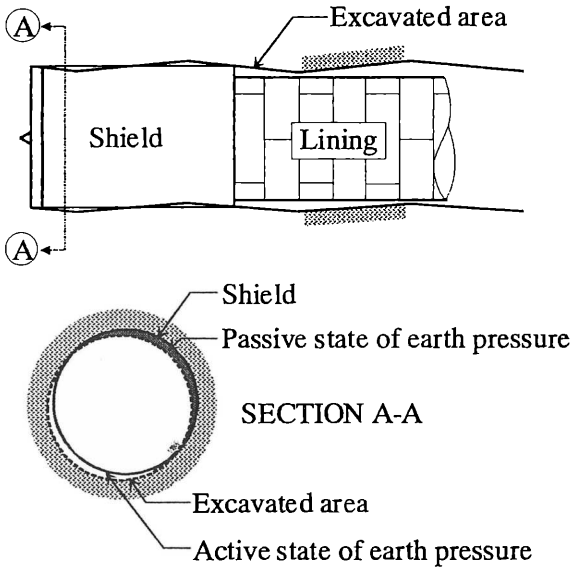

Figure 1. Definition of ground displacement.

2 PROPOSED GROUND REACTION CURVE

The earth pressure distribution on the shield skin plate will play an important role in determining control of the advancing shield. The normal earth pressure acting on the shield periphery is increased or decreased according to the displacement in the surrounding ground due to the shield behaviour (Sugimoto 1994). Based on this concept, a new ground reaction curve was proposed, as shown in Figure 2, taking account of the following conditions:

1. The ground reaction curve is presented by the normal ground displacement of the surrounding ground, U_n, and the coefficient of earth pressure, K_i (i = h, v), where K_h and K_v are the coefficient of earth pressure in the horizontal and vertical directions respectively.

2. K_h and K_v are independent from each other and the coefficient of earth pressure in any direction, K_θ, can be interpolated by using K_h and K_v.

3. K_i has a upper limit, $K_{i\max}$, and a lower limit, $K_{i\min}$, according to large ground deformations as indicate below:

$$\lim_{U_n \to \infty} K_i(U_n) \to K_{i\max} \qquad (i = h, v) \tag{1}$$

$$\lim_{U_n \to -\infty} K_i(U_n) \to K_{i\min} \qquad (i = h, v) \tag{2}$$

4. K_i is equal to the initial coefficient of earth pressure at $U_n = 0$.

$$K_i(U_n = 0) = K_{io} \qquad (i = h, v) \tag{3}$$

where K_{ho} is the coefficient of earth pressure at rest, K_{vo} is the initial coefficient of vertical earth pressure, normally equal to 1.

5. The slope of K_i at U_n = 0 shows the ratio between the coefficient of subgrade reaction, k_i, and the initial vertical earth pressure, σ_{vo}.

$$\frac{\partial K_i(U_n)}{\partial U_n} = \frac{k_i}{\sigma_{vo}} = a_i \qquad \text{at } U_n = 0 \quad (i = h, v) \tag{4}$$

6. The gradient of K_i vs U_n is greatest at U_n = 0, that is,

$$\frac{\partial^2 K_i(U_n)}{\partial U_n^2} = 0 \qquad \text{at } U_n = 0 \quad (i = h, v) \tag{5}$$

Therefore, the proposed new ground reaction curve can be expressed as follows:

For $U_n \le 0$

$$K_h(U_n) = (K_{ho} - K_{h\min}) \tanh\left[\frac{a_h U_n}{K_{ho} - K_{h\min}}\right] + K_{ho} \tag{6}$$

$$K_v(U_n) = (K_{vo} - K_{v\min}) \tanh\left[\frac{a_v U_n}{K_{vo} - K_{v\min}}\right] + K_{vo} \tag{7}$$

For $U_n \ge 0$

$$K_h(U_n) = (K_{ho} - K_{h\max}) \tanh\left[\frac{a_h U_n}{K_{ho} - K_{h\max}}\right] + K_{ho} \tag{8}$$

$$K_v(U_n) = (K_{vo} - K_{v\max}) \tanh\left[\frac{a_v U_n}{K_{vo} - K_{v\max}}\right] + K_{vo} \tag{9}$$

$$K_\theta(U_n, \theta) = K_v(U_n)\cos^2\theta + K_h(U_n)\sin^2\theta \tag{10}$$

where a_h and a_v are the gradient of functions K_h and K_v at U_n=0 respectively and θ is the angle measured from the vertical direction to U_n. The unknown parameters in Equations (6)-(9) can be determined by using the maximum and the minimum of coefficient of earth pressure, the coefficient of earth pressure at rest and the coefficient of subgrade reaction. The earth pressure normal to the skin plate of the shield, σ_n, can be estimated from

$$\sigma_n = K_\theta(U_n, \theta)\sigma_{vo} \tag{11}$$

The value of U_n is calculated by taking account of the shield tunneling excavation condition, the shield movement direction and the position and rotation of the shield. The position, the rotation and the movement direction of the shield are obtained from automatic alignment control system, which consists of a gyrocompass, inclinometer, water level, jack stroke counter and total station.

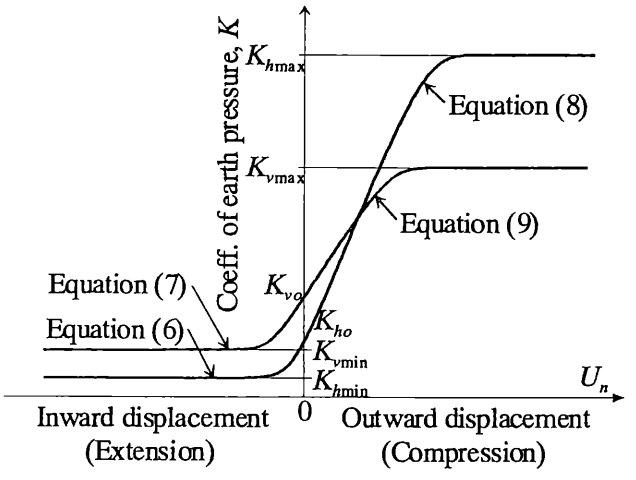

Figure 2. Proposed ground reaction curve.

3 FINITE ELEMENT ANALYSIS

The finite element (FE) studies were devoted to studying the effects of different movement directions of the shield. Using the FE analysis package, CRISP (Britto & Gunn 1987), plane strain conditions were adopted in this study. The linear elastic-perfectly plastic model, with the Mohr-Coulomb failure criteria, was used to model the response of the ground. Six-noded Linear Strain Triangle (LST) and eight-noded Linear Strain Quadrilateral (LSQ) were used to represent the ground. To model the interface between the soil and shield, the interface element, which is a flat eight-noded quadrilateral element with linear elastic properties, was used. The transverse section plane strain model was adopted to model the tunnel, which is perpendicular to the tunnel axis so that the undeformed tunnel appears as a circle in the FE mesh. In-situ stresses were initially established in the mesh.

The shield behaviour was simulated by applying displacements to the shield periphery, where the shield was assumed to be a rigid body. Enforced displacements were applied incrementally at the shield periphery until the shield periphery achieved the specified displacement. The parameters, in Equations (6)-(9), can be obtained by fitting the ground reaction curve with the FE analysis results by Least Square Method (LSM).

4 ANALYSIS OF PARAMETERS IN GROUND REACTION CURVE

The shield tunnelling site test was carried out by using an earth pressure balanced (EPB) shield with

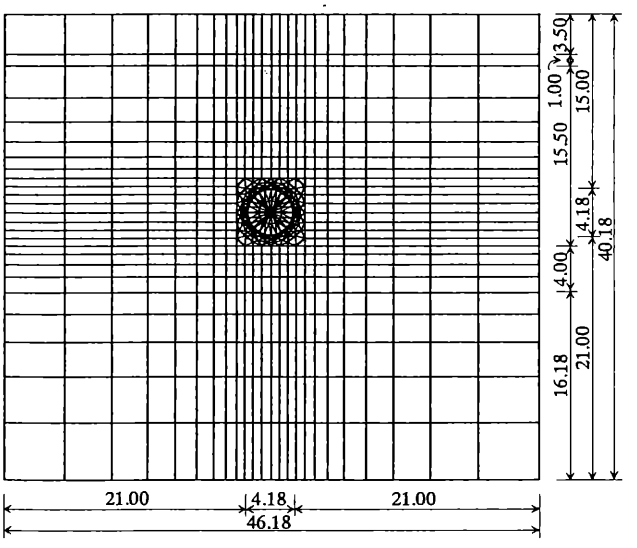

Figure 3. Finite element mesh for shield tunnel (all dimensions are in meters).

Table 1. Soil parameters for FE analysis.

Soil Type	Depth (m)	ϕ (°)	c (KPa)	K_{ho}	ν	E (MPa)
Soft clay	0.0-3.5	–	24	0.60	0.49	7
Sandy gravel (above GW)	3.5-4.5	30	–	0.50	0.33	20
Sandy gravel (below GW)	4.5-20.0	40	–	0.35	0.26	100
Clayey sand	20.0-24.0	10	130	0.40	0.49	65
Clayey gravel	Below 24.0	40	–	0.35	0.26	100

4.18 m outer diameter. The overburden depth was about 15 m and the tunnel was excavated in a sandy gravel layer throughout the site test. The FE mesh was generated using 758 nodes and 856 elements as shown in Figure 3 and the soil parameters in these analyses are shown in Table 1.

Results from the FE analysis for the unlined tunnel indicate that the most of the strain occur near the tunnel opening and are largely restricted to a zone near the excavation surface of the tunnel as shown in Figure 4(*a*). The patterns for the horizontal and vertical strain are very similar but have opposite sign. The pattern of shear strain shows that the shoulder and haunch level of the tunnel is the major shearing zone. The FE analysis results are illustrated in Figures 4(*b*)-4(*f*) for shield movements in direction 0°, 45°, 90°, 135° and 180° measured from the invert of the tunnel in the counter-clockwise direction respectively. The deviation of the shield in each movement direction was assumed to be 5 cm. Thus, the applied displacement at the outer node of the shield in the shield movement direction was 5 cm normal to the shield periphery and for the other outer circumference nodes of the shield, the displacement were applied based on the assumption that the shield is rigidly moved. Figures 4(*b*)-4(*f*) show that most of the strain occurred near the shield periphery and was largely restricted to the active state zone due to the skin plate of the shield detached from the ground. The patterns of both the horizontal and vertical strain are very similar, but have the opposite sign. And the pattern of shear strain is developed in the soil around the tunnel shoulder and haunch level. Figures 4(*b*)-4(*f*) also show that the components of strain in the active state area are almost larger than those in the passive state area.

From FE analysis results of shield excavation, the maximum coefficient of subgrade reaction was found at the spring line of tunnel as shown in Figure 5. The relationships between the coefficients of earth pressure and the ground displacements according to the change of shield position, which are obtained from the FE analysis, are plotted in Figure 6. The fitting of the ground reaction curve to FE analysis results was carried out by applying the Least Square Method as shown in Figure 6. Figure 6 also shows

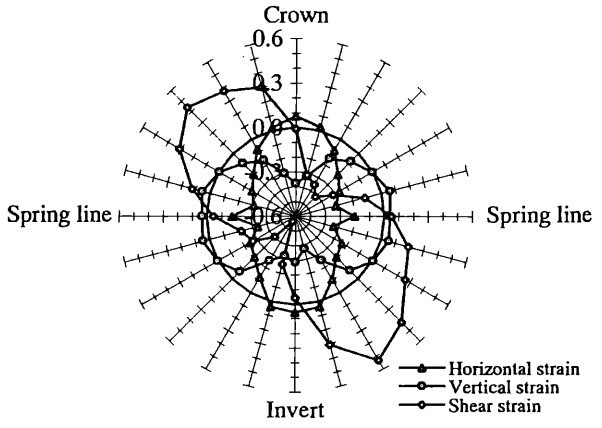

(*a*) Unlined tunnel

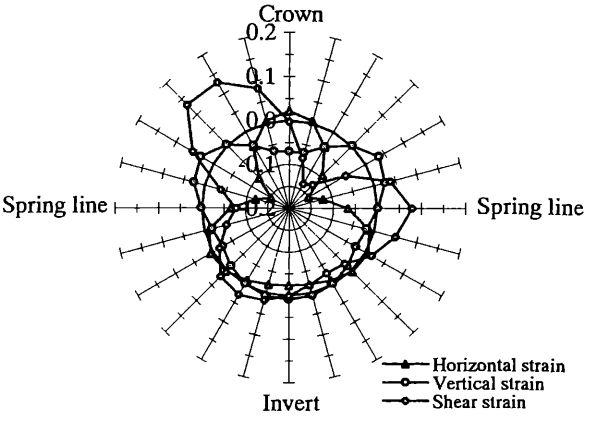

(*b*) Shield movement 0°

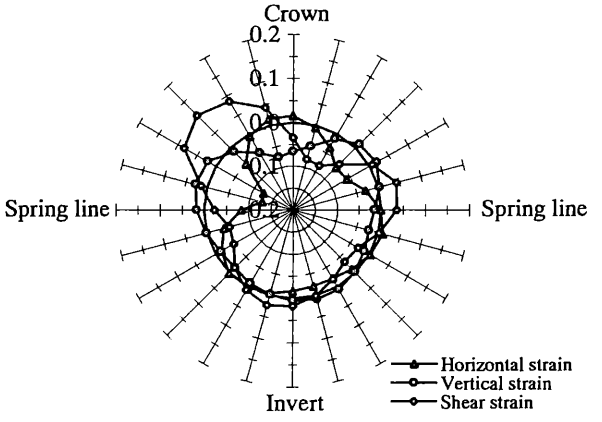

(*c*) Shield movement 45°

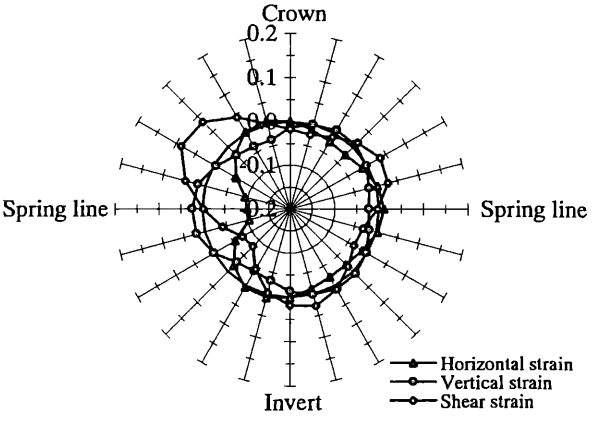

(*d*) Shield movement 90°

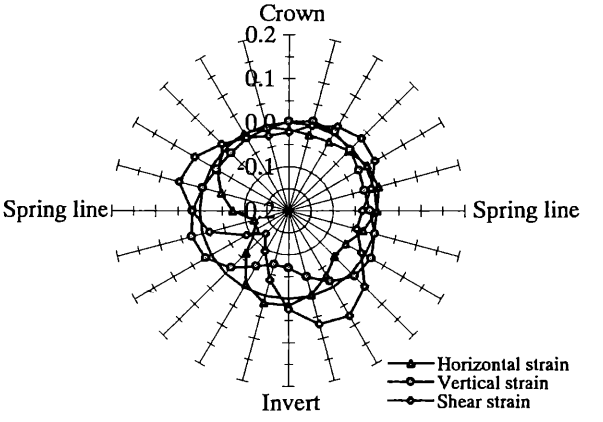

(*e*) Shield movement 135°

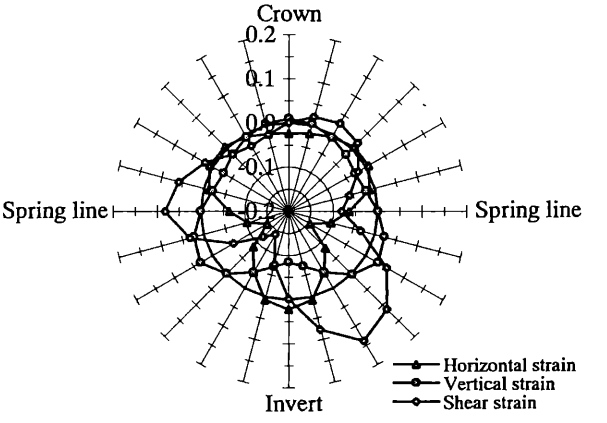

(*f*) Shield movement 180°

Figure 4. Strain around shield tunnel.

that the proposed ground reaction curves has a good agreement with the FE analysis results.

5 PREDICTED GROUND RESPONSE

The proposed ground reaction curve with the obtained parameters from Figure 6 was applied to the 3-D shield behaviour model (Sugimoto & Luong 1996) as the spring characteristic. The spring is normal to the shield skin plate and creates the normal earth pressure acting on the shield skin plate due to the ground deformation. By using this model, the ground response was predicted based on the precise real time measured data of the shield position and rotation with approximately 10 cm interval in the special site test, where the shield was excavated almost in a horizontal straight line. For an example, the normal ground displacement around the shield at data No. 70 is shown in Figure 7. Figure 8 shows the

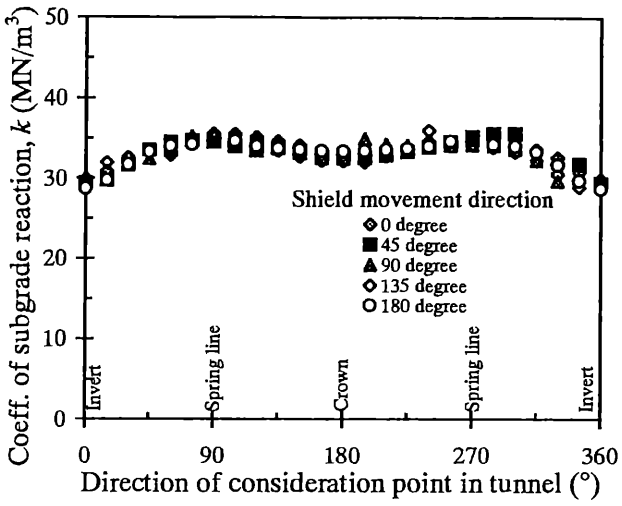

Figure 5. Coefficient of subgrade reaction.

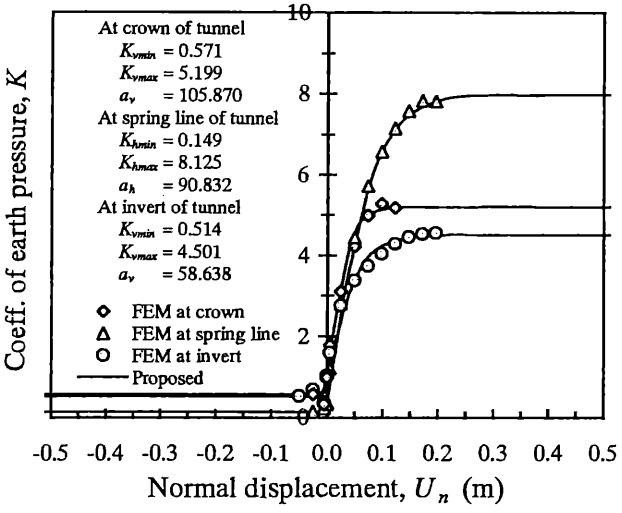

Figure 6. Fitting ground reaction curve to FE analysis.

initial normal earth pressure around the shield periphery before excavation. The normal earth pressure acting on shield predicted by the proposed ground reaction curve is plotted in Figure 9. To make clear the shape of the distribution of the normal ground displacement and the normal earth pressure around the shield, the normal ground displacement and the normal earth pressure on the cross section of the shield, at 0.16 m from the shield tail for data No. 70 are shown in Figures 10-11 respectively. Figures 10-11 correspond to Figures 7, 9 respectively. Figure 7, 9 show that the normal earth pressure change is proportional to the change of ground displacement. The earth pressure acting on shield decreases with the extension of the ground near the shield, while the compressed surrounding ground causes the increase of earth pressure.

The predicted total earth pressure normal to the crown of shield and the observation data obtained by

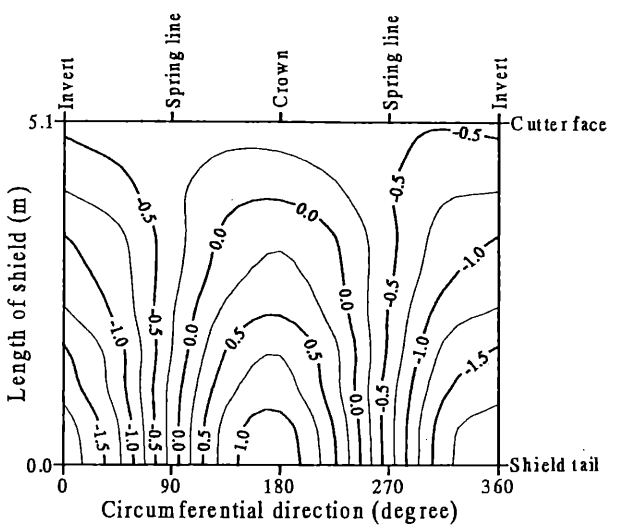

Figure 7. Normal ground displacement around the shield at data No. 70 (cm).

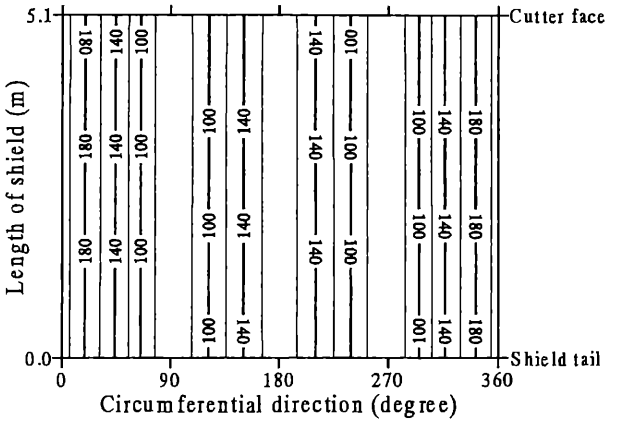

Figure 8. Initial effective normal earth pressure around the shield at data No. 70 (kN/m^2).

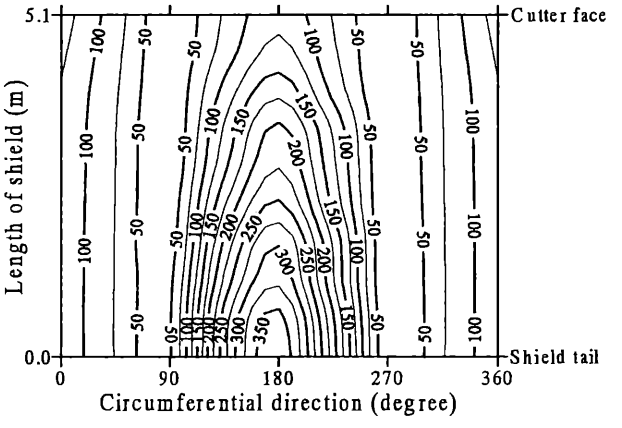

Figure 9. Effective normal earth pressure around the shield at data No. 70 (kN/m^2).

the earth pressure gauge attached at 1.50 m from the cutter face on the crown of shield are compared in Figure 12. Figure 12 shows that the predicted earth

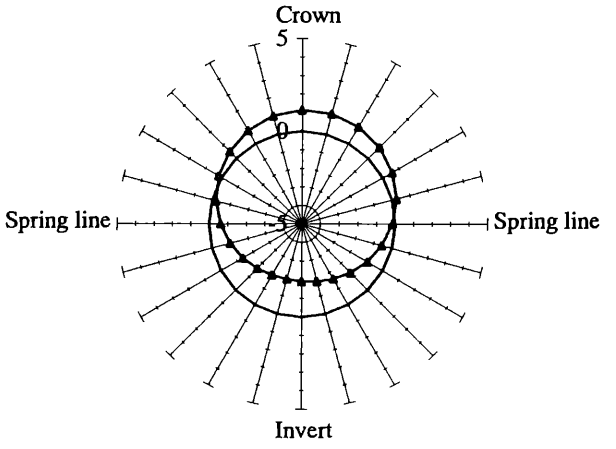

Figure 10. Normal ground displacement around the shield at data No. 70 (0.16 m from shield tail)(cm).

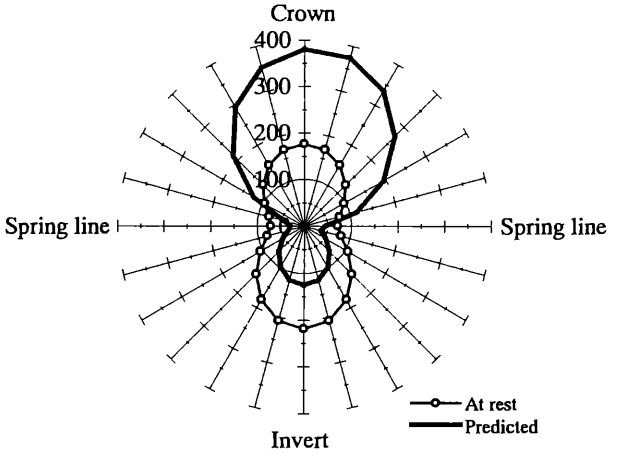

Figure 11. Effective normal earth pressure acting on shield at data No. 70 (0.16 m from shield tail)(kN/m^2).

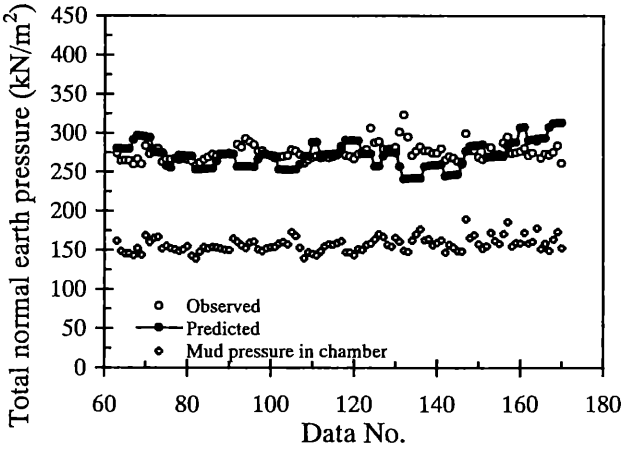

Figure 12. Predicted and observed total normal earth pressure acting on the crown of shield.

pressure is close to the observation data, though there is some variation caused by the change of ground displacement due to the shield movement.

6 CONCLUSIONS

This paper presents a simplified ground reaction curve that is applicable for the shield tunnelling method. This ground reaction curve was developed in conjunction with 2-D FE analysis. From the FE analysis results, it was found that the state of earth pressure around the shield during excavation depend on the over-excavation, the position and the rotation of shield, and the shield movement direction. The proposed ground reaction curve provides a reasonable estimate of earth pressure in applying it to the shield model. This proposed curve could also be applied to tunnel lining design as well as to subsurface structures where similar conditions are considered.

ACKNOWLEDGEMENT

This research was supported by the Program for Promoting Fundamental Transport Technology Research from the Corporation for Advanced Transport & Technology (CATT).

REFERENCES

Britto, A.M. & M.J. Gunn. 1987. *Critical State Soil Mechanics via Finite Elements*, Ellis Horwood, Chichester.

Sugimoto, M. 1994. Modeling of loads acting on shield. In K. Fujita & O. Kusakabe (eds), *Proc. Int. Symposium on Underground Construction in Soft Ground*: 273-276. Rotterdam : Balkema.

Sugimoto, M. & N.T.H. Luong 1996. Soil properties based on in-situ data of shield driven method. In R.J. Mair & R.N. Taylor (eds), *Proc. Int. Symposium on Geotechnical Aspects of Underground Construction in Soft Ground*: 607-612. Rotterdam : Balkema.